order of the phase-integral approximations to be used in the definition (14) of $L(E)$, we may expect formulas (15) and (16) to be very accurate.

IV. FERMI-SEGRE FORMULA

In accordance with the quantization condition (15) we now replace $[(\partial/\partial E)L(E)]_{E=E_n}$ by $\pi(dn/dE_n)$, i.e., by $\pi/(dE_n/dn)$. In this way we obtain from (16) the nonrelativistic Fermi–Segrè formula

$$\psi_n^2(0) = \frac{Z}{\pi a_0^2 e^2}\frac{dE_n}{dn} \quad , \tag{18}$$

where dE_n/dn is to be obtained by means of spectroscopic data.

Like formulas (15) and (16), also the nonrelativistic Fermi–Segrè formula (18) is exact in the particular cases of the attractive, pure-Coulomb potential and of the potential (17).

Recalling what was said at the end of Sec. III about the accuracy of formulas (15) and (16), we may draw the following conclusion as to the accuracy and applicability of the nonrelativistic Fermi–Segrè formula (18). If the idealized model used in the present paper were physically realistic, i.e., if it were completely justified to use the one-particle model with a nonrelativistic s electron moving in a local potential, which in a certain region around $r = 0$ is approximately a Coulomb potential due to a point-shaped nucleus of charge number Z, then the essential limitation for the accuracy of the nonrelativistic Fermi–Segrè formula should be connected to the possibility of calculating de_n/dn by interpolation from the spectroscopic term values. For unperturbed terms this calculation has been discussed by Crawford and Schawlow on p. 1312 in Ref. 3.

[1]E. Fermi and E. Segrè, *Reale Accademia d'Italia, Memorie della classe di Scienze Fisiche, Matematiche e Naturali* (Reale Accademia d'Italia, Roma, 1933), Vol. IV, pp. 131–158.
[2]E. Fermi and E. Segrè, Z. Physik 82, 729 (1933).
[3]M. F. Crawford and A. L. Schawlow, Phys. Rev. 76, 1310 (1949).
[4]L. L. Foldy, Phys. Rev. 111, 1093 (1958).
[5]N. Fröman and P. O. Fröman, *JWKB Approximation, Contributions to the Theory* (North-Holland, Amsterdam, 1965).
[6]N. Fröman, Arkiv Fysik 32, 541 (1966).
[7]N. Fröman, Ann. Phys. (N. Y.) 61, 451 (1970).
[8]W. H. Furry, Phys. Rev. 71, 360 (1947).
[9]S. Yngve, J. Math. Phys. 13, 324 (1972).
[10]Private communication from Dr. J. A. Campbell, Center for Particle Theory and Department of Computer Science, University of Texas at Austin, Austin, Texas 78712.
[11]L. Hulthén, Arkiv Mat. Astron. Fysik 28A, No. 5 (1942).

PHYSICAL REVIEW A VOLUME 6, NUMBER 6 DECEMBER 1972

Determination of Mass-Attenuation Coefficients in Krypton and Xenon by Continuous Analysis between 8 and 0.8 keV

François Wuilleumier
Laboratoire de Chimie Physique de la Faculté des Sciences de Paris, Paris, France
(Received 1 May 1972)

The bremsstrahlung emitted from a tungsten anode in an x-ray tube has been used for continuous analysis of krypton and xenon absorption spectra between 8 and 0.8 keV (1.5 to 15 Å). Attenuation coefficients were determined every 0.05 Å between 1.5 and 8 Å (in steps of energy varying from 150 to 10 eV) and every 0.1 Å between 8 and 15 Å (20 to 5 eV). Results obtained are compared with previously determined experimental values and with semiempirical and theoretical determinations. Tabulated data of McMaster *et al.* and calculations of McGuire are shown to be in good agreement with the experimental results, generally within 10%. Multiply excited and ionized states have been observed in krypton, owing to simultaneous interaction of incident radiation with $2p$ and $4p$ (and $4s$) electrons, and a nonhydrogenic behavior of the xenon $3p$-subshell photoionization cross section has been revealed. Krypton and xenon L and xenon M_{III} absorption jump ratios have been determined. Finally, continuous oscillator strengths of krypton and xenon L shells and the xenon M shell have been evaluated.

I. INTRODUCTION

Until about 1960 all x-ray attenuation-coefficient measurements were performed using x-ray characteristic lines as radiation sources. The various semiempirical methods elaborated for attenuation-coefficient determinations (Jönsson,[1] Victoreen,[2] Henke *et al.*,[3] Leroux,[4] and Heinrich[5]) were thus based on a few discrete data points for each element. Using synchroton radiation has made possi-

ble, in the ultrasoft x-ray region, a continuous analysis in energy of the attenuation coefficients. Nonhydrogenic behavior of subshell photoionization cross sections has thus been revealed in heavy elements[6] by such an analysis, in agreement with theoretical calculations.[7] A great number of absorption lines, appearing in spectra as more or less weak variations of attenuation coefficients, have also been discovered in rare gases[8] and attributed to single- and multiple-excitation processes. At the same time also, Lukirskii[9] developed a method of using bremsstrahlung emitted by an x-ray tube in the ultrasoft x-ray region.

In the soft x-ray region (1 to 10 keV), we were the first to carry out such an analysis in neon and argon, by using bremsstrahlung emitted from an x-ray tube operated with a tungsten anode.[10] We have done similar measurements in krypton and xenon. Results related to discrete single and multiple processes have already been published.[11] We will present here attenuation coefficients measured in gaseous krypton and xenon by continuous energy analysis of their absorption spectrum. In the whole energy range of this study (0.8–8 keV), only a few attenuation coefficients have been measured in these elements by means of characteristic lines. The only similar studies have been carried out by Senemaud[12] in beryllium and carbon, and by McCrary *et al.*[13] for metals in a higher energy range (25–130 keV). We will also compare our results with McGuire's calculations[14] using Herman and Skillman's central potential,[15] with various semiempirical determinations and with recently tabulated data in compilations of Storm and Israel[16] and McMaster *et al.*[17] Finally we will give krypton and xenon L jump ratios and continuous oscillator strengths.

II. APPARATUS

The narrow-beam mass-attenuation coefficient μ/ρ in units of cm^2/g is defined by the relation

$$I/I_0 = e^{-(\mu/\rho)x}, \tag{1}$$

where I/I_0 is the gas transmissivity and x is the sample thickness in g/cm^2.

The apparatus has been described in detail elsewhere.[18] We will only recall its essential characteristics.

A Johann vacuum spectrograph with a 50-cm bent crystal was used for the measurements. Various crystals (quartz, gypsum, mica) allowed us to cover the whole energy range. Bremsstrahlung emitted from W or Pt anodes in an x-ray tube was filtered through two 0.5-μm Al foils or one 25-μm Be foil, according to the x-ray energy. Several characteristic x-ray lines served to calibrate energy in the spectrum. The tube was powered by a 12-kV 100-mA power supply. The high voltage and current stabilization were, respectively, better than 2×10^{-4} and 10^{-3}. 500 W of power was usually dissipated in the anode.

Continuous coverage of the energy range was assured by a photographic detection. The film was placed in a holder, kept tangent to the focalization circle and equipped with a shutter which could be moved along the height of the film, delineating six positions noted P_1 to P_6. Different types of films were used: Kodak Difrax above 1.2 keV, Kodak Spectrum Analysis No. 3 and DC3 below 1.2 keV. The film responses $d=f(I)$ (where d is the optical density and I the radiation flux) have been determined[18,19] in the whole energy range. A Joyce Loelb microdensitometer was used for analysis of the films.

The gas was introduced in a small cell located between the x-ray tube window and the crystal. This location had been shown[20] to be the best for narrow-beam-attenuation measurements, because most of the secondary radiations, emitted or scattered in the gas, cannot reach the detector. Three cells of different lengths were used, according to the Bragg angle of each experiment. Two apertures in the walls of the cell allowed the radiation to be transmitted to the crystal. Depending on the energy of the radiation, they were covered with 6- or 4-μm Mylar foils or 2-μm Makrofol foils which were able to keep in the cell a pressure of several hundred Torr without leaking. The sizes of these apertures had been calculated so that all the radiation passing through the cell can only reach the crystal and be reflected. The solid angle thus delineated was about 10^{-2}. The gas pressure was measured by means of an oil manometer using low vapor pressure (10^{-8} Torr) and low-viscosity silicon oil. The gas temperature was measured with a thermocouple.

Samples of research grade noble gases were purchased commercially. Quantitative analysis performed by the vendor indicated that the gases had the following purities: krypton 99.95%, xenon 99.95%.

III. EXPERIMENTAL PROCEDURE

The geometrical width of the spectrum for each run was about 40 mm, corresponding to an energy width from 40 to 400 eV; this energy range will be called hereafter the partial energy range. Each crystal could be adjusted at Bragg angles ranging from 30° to 65°, and five different crystals allowed us to cover the whole energy range as indicated in Table I. Also given are the reference lines used to calibrate in energy the spectra.

For each partial energy range, six spectra were recorded on the positions P_1 to P_6. They were taken in the following sequence: unattenuated photon beam intensity, attenuated intensity by a certain

TABLE I. Summary of experimental conditions.

Wavelength range (Å)	Energy range (keV)	Crystal		d_1 (*ux*)	Reference lines
1.5–2.5	8.3–5.0	Quartz	0001	1797.79[a]	(Cr-*V*-Fe)$K\alpha_1\beta_1$ in first order
2.1–4.5	6.0–2.7	Quartz	$11\bar{2}0$	2451.23[b]	(Cr-*V*-Ti)$K\alpha_1\beta_1$ (Sn-Ag-Pd)$L\alpha_1\beta_1$ in first order
4.0–7.6	3.1–1.6	Quartz	$10\bar{1}0$	4244.91[a]	(Nb to Ag)$L\alpha_1\beta_1$ in first and second orders
7.0–13.5	1.7–0.9	Gypsum	010	7579.07[c]	(Nb to Ag)$L\alpha_1\beta_1$ in second and third orders (Cr-*V*-Ti)$K\alpha_1$ in fourth order
10.0–15.0	1.2–0.8	Mica	002	9927.58[c]	(Ru to Ag)$L\alpha_1\beta_1$ (Ti to Cr)$K\alpha_1\beta_1$ in fifth order

[a]Reference 21.
[b]Reference 22.
[c]Reference 23.

gas pressure, unattenuated intensity, attenuated intensity with another pressure, unattenuated intensity, reference lines. Exposure times for unattenuated beam varied from 15 min to 5 h, the x-ray-tube high voltage being kept lower than twice the smallest energy of the partial energy range under study. The pressures in the gas cell were selected to give a value of I/I_0 from 0.1 to 0.4, thus varying from 7 to 100 Torr. Exposure times for attenuated beams were adjusted in order to get similar optical densities for all spectra recorded on the same film. The gas pressure and temperature were continuously measured during each run.

Recording of unattenuated beam intensity on the whole film without shutter allowed us to determine an intensity correction factor for each position; the x-ray-tube emission was checked to be steady by successively recording, in the same conditions, the unattenuated beam at each position.

For each partial energy range three to five complete sequences were recorded. Sample lengths, pressures, and recording positions of unattenuated and attenuated intensities were changed between each sequence. Finally, ten densitograms were recorded for each film with the microdensitometer.

IV. DATA ANALYSIS

From the continuous transmission curves on the densitograms the attenuation coefficients were calculated every 0.05 Å between 1.5 and 8Å (in steps of energy varying from 150 to 10 eV) and every 0.1 Å between 8 and 15 Å (20 to 5 eV).

The energy scale on each densitogram was determined from the two reference lines recorded by using Haglund's formula.[24] The wavelengths of the lines in kxu (kilo x units) were taken from Cauchois and Hulubei's table.[25] The wavelengths were converted to energies by the relation[26]

$$E(\text{eV})\,\lambda(\text{kxu}) = 12\,372.855\ .$$

The optical densities measured were related to radiation flux intensities I_0 and I by means of the measured film-response function. The value of I_0 used was the mean of the unattenuated beam intensities measured before and after recording the attenuated beam. Using the ratio I/I_0 thus determined and P and T measured, attenuation coefficients were calculated by means of relation (1) which can be written, considering krypton and xenon as perfect gases,

$$\frac{\mu}{\rho_{(\text{cm}^2/\text{g})}} = \frac{1}{\rho_0 l}\,\frac{P_0}{P}\,\frac{T}{T_0}\ln\frac{I_0}{I}\ , \tag{2}$$

where ρ_0 is the density of the gas STP, l is the length of the cell, P_0 and T_0 are STP values, namely, 760 mm Hg and 273.15 °C, P and T are the measured pressure and absolute temperature, respectively. The values of ρ_0 used were 3.733×10^{-3} g/cm^3 for krypton and 5.887×10^{-3} g/cm^3 for xenon.[27] For the pressures and temperatures used in these experiments, the error introduced by assuming the validity of the perfect-gas law was negligible.

Possible sources of error in the experimental measurements include the following: beam intensity measurements, sample characteristics (length, pressure, and temperature), gas purity, and finite geometry.

Beam intensity measurements. Errors in μ/ρ due to electronic variations are negligible (~0.1%) because of the high degree of tube-voltage and tube-current stabilization. Errors due to optical density measurements are the most important. They can introduce an uncertainty of 3 to 4% in each independent attenuation-coefficient determination. The high number of measurements for each attenuation coefficient significantly reduced the effects of this factor.

Sample characteristics. Errors due to cell-length measurements were between 0.6 to 1.1%, according to the cell used. Errors in μ/ρ due to temperature and pressure measurements were, respectively, about 0.1% and 0.15 to 0.65%.

Gas purity. Errors in μ/ρ due to sample impurities were less than 0.1% for all the measurements.

Finite geometry. Small-angle scattering of photons to the crystal and multiple Compton scattering by the chamber walls and gas would tend to lower the measured attenuation coefficients. However, the position of the absorption cell between the x-ray tube and the crystal, the narrow-beam geometry, and the very low total scattering cross section, less than 1% in almost all the energy range, make this source of errors negligible.

Maximum errors in independent determination of μ/ρ can reach almost 6%. However, applying least-squares methods to the ten values determined for each attenuation coefficient allowed us to obtain a standard deviation of 1 to 2% for most of the energies.

Error in the energies. The method of determining the energy scale and the accuracy of reading the densitograms lead to errors on the energies varying from 0.8 eV at high energy to 0.06 eV at low energy; this represents an almost constant relative error of about 10^{-4}.

V. RESULTS

The results of the experimental measurements are listed in Table II. Columns 1 and 2 give λ in kxu and the corresponding energy E in eV. Columns 3 and 5 give measured attenuation coefficients for krypton and xenon in cm^2/g. The quoted errors are twice the standard deviation, giving the 95%

TABLE II. Experimentally determined values of x-ray attenuation coefficients in krypton and xenon.

λ kxu	E eV	Krypton $\mu/\rho(10^2\ cm^2/g)$	Krypton $\sigma(10^4$ b/atom)	Xenon $\mu/\rho(10^2\ cm^2/g)$	Xenon $\sigma(10^5$ b/atom)
1.500	8248.6	0.97 ± 0.04	1.32	2.75 ± 0.12	0.59
1.550	7982.3	1.02 ± 0.05	1.39	3.00 ± 0.13	0.65
1.600	7733.1	1.10 ± 0.05	1.49	3.27 ± 0.10	0.70
1.650	7498.6	1.21 ± 0.05	1.64	3.54 ± 0.13	0.76
1.700	7278.2	1.28 ± 0.06	1.74	3.83 ± 0.17	0.84
1.750	7070.2	1.42 ± 0.04	1.94	4.15 ± 0.15	0.90
1.800	6873.8	1.53 ± 0.06	2.09	4.47 ± 0.17	0.97
1.850	6688.0	1.64 ± 0.06	2.24	4.81 ± 0.13	1.05
1.900	6512.0	1.77 ± 0.08	2.42	5.18 ± 0.23	1.12
1.950	6345.0	1.88 ± 0.09	2.58	5.53 ± 0.22	1.20
2.000	6186.4	2.02 ± 0.11	2.77	5.92 ± 0.28	1.28
2.050	6035.6	2.19 ± 0.13	3.01	6.34 ± 0.22	1.37
2.100	5891.8	2.36 ± 0.12	3.24	6.73 ± 0.23	1.46
2.150	5754.8	2.49 ± 0.11	3.42	7.16 ± 0.27	1.55
2.200	5624.1	2.63 ± 0.12	3.62	7.62 ± 0.31	1.65
2.250	5499.1	2.82 ± 0.15	3.87	8.17 ± 0.31	1.77
Xe	5452.8$^+$			8.35 ± 0.31	1.59
L_{I}	5452.8$^-$			7.05 ± 0.23	1.54
2.300	5379.5	2.98 ± 0.17	4.10	7.25 ± 0.23	1.57
2.350	5265.0	3.16 ± 0.16	4.35	7.36 ± 0.31	1.59
2.400	5155.4	3.35 ± 0.11	4.61	7.92 ± 0.29	1.72
Xe	5103.9$^+$			8.20 ± 0.30	1.79
L_{II}	5103.9$^-$			5.99 ± 0.21	1.31
2.450	5050.1	3.54 ± 0.15	4.88	6.15 ± 0.23	1.33
2.500	4949.1	3.72 ± 0.16	5.13	6.25 ± 0.27	1.35
2.550	4852.1	3.92 ± 0.21	5.40	6.32 ± 0.29	1.37
Xe	4782.5$^+$			6.60 ± 0.23	1.44
L_{III}	4782.5$^-$			2.31 ± 0.09	0.50
2.600	4758.8	4.11 ± 0.17	5.67	2.32 ± 0.11	0.50
2.650	4669.0	4.35 ± 0.22	6.00	2.44 ± 0.10	0.52
2.700	4582.6	4.54 ± 0.23	6.27	2.55 ± 0.14	0.55
2.750	4499.3	4.77 ± 0.19	6.59	2.67 ± 0.15	0.57
2.800	4418.8	5.01 ± 0.22	6.92	2.75 ± 0.18	0.59
2.850	4341.3	5.23 ± 0.17	7.23	2.92 ± 0.16	0.63
2.900	4266.5	5.48 ± 0.23	7.57	3.03 ± 0.14	0.65
2.950	4194.2	5.74 ± 0.24	7.94	3.14 ± 0.11	0.68
3.000	4124.3	6.00 ± 0.32	8.30	3.28 ± 0.14	0.71
3.050	4056.7	6.28 ± 0.26	8.69	3.42 ± 0.11	0.74
3.100	3991.3	6.53 ± 0.21	9.03	3.57 ± 0.15	0.77
3.150	3927.9	6.82 ± 0.22	9.49	3.73 ± 0.12	0.80
3.200	3866.5	7.12 ± 0.29	9.91	3.88 ± 0.14	0.84
3.250	3807.0	7.40 ± 0.38	1.03×10^5	4.05 ± 0.15	0.87
3.300	3749.3	7.61 ± 0.32	1.06	4.21 ± 0.18	0.91
3.350	3693.4	7.83 ± 0.33	1.09	4.38 ± 0.23	0.95
3.400	3639.1	8.09 ± 0.25	1.13	4.54 ± 0.20	0.98
3.450	3586.4	8.40 ± 0.34	1.17	4.73 ± 0.22	1.02
3.500	3535.1	8.70 ± 0.36	1.21	4.91 ± 0.19	1.06

TABLE II. (*Continued*)

λ	E	Krypton		Xenon	
kxu	eV	$\mu/\rho(10^3\ \mathrm{cm}^2/\mathrm{g})$	$\sigma(10^5$ b/atom)	$\mu/\rho(10^2\ \mathrm{cm}^2/\mathrm{g})$	$\sigma(10^5$ b/atom)
3.550	3485.3	0.90 ± 0.05	1.26	5.11 ± 0.18	1.10
3.600	3437.0	0.93 ± 0.04	1.30	5.29 ± 0.14	1.14
3.650	3389.8	0.96 ± 0.03	1.34	5.48 ± 0.20	1.18
3.700	3344.0	1.00 ± 0.04	1.39	5.69 ± 0.16	1.23
3.750	3299.4	1.04 ± 0.05	1.44	5.88 ± 0.17	1.27
3.800	3256.0	1.07 ± 0.05	1.49	6.09 ± 0.22	1.32
3.850	3213.7	1.11 ± 0.05	1.55	6.32 ± 0.23	1.37
3.900	3172.5	1.15 ± 0.04	1.60	6.51 ± 0.25	1.41
3.950	3132.4	1.19 ± 0.06	1.66	6.72 ± 0.24	1.46
4.000	3093.2	1.23 ± 0.06	1.72	6.94 ± 0.31	1.50
4.050	3055.0	1.27 ± 0.05	1.77	7.21 ± 0.22	1.56
4.100	3017.8	1.31 ± 0.06	1.82	7.49 ± 0.33	1.62
4.150	2981.4	1.36 ± 0.06	1.89	7.65 ± 0.31	1.66
4.200	2946.0	1.41 ± 0.06	1.96	7.91 ± 0.30	1.71
4.250	2911.3	1.45 ± 0.05	2.02	8.14 ± 0.31	1.76
4.300	2877.5	1.50 ± 0.05	2.08	8.42 ± 0.30	1.83
4.350	2844.3	1.54 ± 0.06	2.15	8.63 ± 0.27	1.87
4.400	2812.0	1.59 ± 0.08	2.22	8.85 ± 0.33	1.92
4.450	2780.5	1.64 ± 0.06	2.29	9.14 ± 0.38	1.98
4.500	2749.5	1.69 ± 0.05	2.36	9.31 ± 0.26	2.02
4.550	2719.3	1.75 ± 0.07	2.43	9.60 ± 0.31	2.08
4.600	2689.7	1.80 ± 0.07	2.51	9.91 ± 0.39	2.15
4.650	2660.8	1.86 ± 0.06	2.59	1.01 ± 0.04	2.19
4.700	2632.5	1.91 ± 0.07	2.66	1.04 ± 0.05	2.25
4.750	2604.8	1.97 ± 0.09	2.74	1.06 ± 0.04	2.29
4.800	2577.7	2.01 ± 0.06	2.80	1.09 ± 0.04	2.38
4.850	2551.1	2.08 ± 0.06	2.89	1.12 ± 0.05	2.43
4.900	2525.1	2.15 ± 0.09	2.98	1.14 ± 0.05	2.48
4.950	2499.6	2.20 ± 0.07	3.06	1.17 ± 0.05	2.54
5.000	2474.6	2.26 ± 0.08	3.14	1.19 ± 0.04	2.57
5.050	2450.1	2.32 ± 0.07	3.23	1.23 ± 0.05	2.66
5.100	2426.1	2.38 ± 0.10	3.30	1.26 ± 0.04	2.73
5.150	2402.5	2.44 ± 0.09	3.39	1.28 ± 0.05	2.78
5.200	2379.4	2.50 ± 0.08	3.48	1.31 ± 0.06	2.85
5.250	2356.8	2.56 ± 0.10	3.56	1.35 ± 0.05	2.92
5.300	2334.5	2.61 ± 0.10	3.63	1.37 ± 0.05	2.99
5.350	2312.6	2.68 ± 0.13	3.73	1.40 ± 0.05	3.05
5.400	2291.2	2.75 ± 0.10	3.83	1.44 ± 0.06	3.12
5.450	2270.4	2.81 ± 0.14	3.91	1.47 ± 0.07	3.20
5.500	2249.6	2.88 ± 0.11	4.01	1.50 ± 0.06	3.27
5.550	2229.3	2.95 ± 0.09	4.10	1.53 ± 0.06	3.32
5.600	2209.4	3.01 ± 0.12	4.19	1.56 ± 0.06	3.39
5.650	2189.9	3.08 ± 0.12	4.29	1.60 ± 0.08	3.48
5.700	2170.7	3.14 ± 0.15	4.37	1.64 ± 0.07	3.55
5.750	2151.8	3.21 ± 0.16	4.47	1.67 ± 0.07	3.64
5.800	2133.2	3.27 ± 0.14	4.55	1.70 ± 0.06	3.71
5.850	2115.0	3.34 ± 0.11	4.65	1.74 ± 0.05	3.78
5.900	2097.1	3.41 ± 0.14	4.75	1.77 ± 0.05	3.85
5.950	2079.5	3.48 ± 0.14	4.84	1.81 ± 0.07	3.93
6.000	2062.1	3.55 ± 0.11	4.94	1.86 ± 0.06	4.03
6.050	2045.1	3.63 ± 0.14	5.04	1.89 ± 0.07	4.10
6.100	2028.4	3.69 ± 0.15	5.13	1.93 ± 0.07	4.19
6.150	2011.9	3.75 ± 0.18	5.22	1.97 ± 0.08	4.28
6.200	1995.6	3.84 ± 0.12	5.34	2.01 ± 0.06	4.36
6.250	1979.7	3.90 ± 0.11	5.43	2.05 ± 0.08	4.46
6.300	1964.0	3.98 ± 0.11	5.54	2.09 ± 0.09	4.55
6.350	1948.4	4.06 ± 0.18	5.65	2.15 ± 0.08	4.66
6.400	1933.4	4.14 ± 0.17	5.76	2.18 ± 0.10	4.74
Kr	1921.6$^+$	4.18 ± 0.17	5.82		
L_{I}	1921.6$^-$	3.64 ± 0.18	5.07		
6.450	1918.3	3.65 ± 0.19	5.08	2.24 ± 0.09	4.86

TABLE II. (*Continued*)

λ kxu	E eV	Krypton $\mu/\rho(10^3$ cm^2/g)	Krypton $\sigma(10^5$ b/atom)	Xenon $\mu/\rho(10^3$ cm^2/g)	Xenon $\sigma(10^5$ b/atom)
6.500	1903.6	3.70 ± 0.18	5.15	2.28 ± 0.09	4.95
6.550	1889.0	3.74 ± 0.19	5.20	2.32 ± 0.07	5.04
6.600	1874.7	3.78 ± 0.19	5.26	2.36 ± 0.10	5.13
6.650	1860.6	3.83 ± 0.17	5.33	2.40 ± 0.10	5.21
6.700	1846.7	3.88 ± 0.12	5.40	2.46 ± 0.10	5.33
6.750	1833.1	3.94 ± 0.16	5.48	2.50 ± 0.08	5.44
6.800	1819.5	3.99 ± 0.15	5.56	2.54 ± 0.11	5.52
6.900	1793.1	4.12 ± 0.20	5.73	2.65 ± 0.10	5.75
6.950	1780.2	4.18 ± 0.17	5.82	2.70 ± 0.10	5.86
7.000	1767.5	4.26 ± 0.18	5.92	2.74 ± 0.11	5.94
7.050	1755.0	4.34 ± 0.13	6.03	2.78 ± 0.11	6.05
7.100	1742.6	4.41 ± 0.13	6.13	2.83 ± 0.12	6.16
7.150	1730.4			2.88 ± 0.09	6.26
Kr	1729.6$^+$	4.48 ± 0.18	6.23		
L_{II}	1729.6$^-$	3.10 ± 0.13	4.31		
7.200	1718.4	3.11 ± 0.15	4.33	2.92 ± 0.11	6.35
7.250	1706.6	3.17 ± 0.12	4.41	2.97 ± 0.09	6.44
7.300	1694.9	3.27 ± 0.15	4.53	3.02 ± 0.10	6.56
7.350	1683.4	3.28 ± 0.10	4.56	3.08 ± 0.09	6.68
Kr	1677.3$^+$	3.32 ± 0.15	4.62		
L_{III}	1677.3$^-$	0.80 ± 0.03	1.11		
7.400	1672.0	0.80 ± 0.03	1.11	3.12 ± 0.10	6.78
7.450	1660.8	0.81 ± 0.04	1.13	3.17 ± 0.12	6.89
7.500	1649.7	0.82 ± 0.04	1.14	3.20 ± 0.10	6.96
7.550	1638.8	0.84 ± 0.04	1.16	3.26 ± 0.13	7.08
7.600	1628.0	0.85 ± 0.04	1.18	3.30 ± 0.14	7.18
7.650	1617.4	0.87 ± 0.03	1.21	3.36 ± 0.11	7.30
7.700	1606.9	0.88 ± 0.03	1.23	3.41 ± 0.13	7.40
7.750	1596.5	0.90 ± 0.03	1.25	3.46 ± 0.11	7.52
7.800	1586.3	0.91 ± 0.04	1.27	3.50 ± 0.14	7.62
7.850	1576.2	0.93 ± 0.04	1.29	3.55 ± 0.13	7.73
7.900	1566.2	0.94 ± 0.05	1.31	3.61 ± 0.10	7.84
7.950	1556.3	0.96 ± 0.04	1.33	3.66 ± 0.12	7.96
8.000	1546.6	0.97 ± 0.04	1.35	3.71 ± 0.15	8.07
8.100	1527.5	1.00 ± 0.05	1.40	3.81 ± 0.15	8.28
8.200	1508.9	1.04 ± 0.06	1.44	3.91 ± 0.20	0.85
8.300	1490.7	1.06 ± 0.05	1.48	4.00 ± 0.16	0.87
8.400	1473.0	1.09 ± 0.06	1.52	4.11 ± 0.19	0.90
8.500	1455.7	1.13 ± 0.05	1.57	4.21 ± 0.17	0.92
8.600	1438.7	1.16 ± 0.05	1.62	4.30 ± 0.17	0.94
8.700	1422.2	1.20 ± 0.05	1.67	4.41 ± 0.21	0.96
8.800	1406.0	1.24 ± 0.06	1.72	4.51 ± 0.22	0.98
8.900	1390.2	1.27 ± 0.06	1.77	4.60 ± 0.25	1.00
9.000	1374.8	1.31 ± 0.05	1.82	4.70 ± 0.24	1.03
9.100	1359.7	1.32 ± 0.05	1.84	4.80 ± 0.24	1.05
9.200	1344.9	1.38 ± 0.06	1.93	4.91 ± 0.25	1.07
9.300	1330.5	1.41 ± 0.07	1.96	5.01 ± 0.21	1.09
9.400	1316.3	1.46 ± 0.08	2.04	5.11 ± 0.22	1.11
9.500	1302.4	1.51 ± 0.07	2.10	5.20 ± 0.25	1.13
9.600	1288.8	1.54 ± 0.08	2.15	5.30 ± 0.21	1.16
9.700	1275.5	1.58 ± 0.06	2.20	5.42 ± 0.22	1.18
9.800	1262.5	1.63 ± 0.07	2.26	5.51 ± 0.23	1.20
9.900	1249.7	1.67 ± 0.08	2.32	5.61 ± 0.23	1.22
10.000	1237.2	1.71 ± 0.10	2.37	5.72 ± 0.28	1.25
10.100	1225.0	1.75 ± 0.10	2.43	5.82 ± 0.24	1.27
10.200	1213.0	1.80 ± 0.09	2.50	5.92 ± 0.24	1.29
10.300	1201.2	1.84 ± 0.09	2.57	6.02 ± 0.35	1.31
10.400	1189.7	1.89 ± 0.11	2.62	6.12 ± 0.25	1.33
10.500	1178.3	1.93 ± 0.10	2.68	6.22 ± 0.31	1.36
10.600	1167.2	1.98 ± 0.08	2.75	6.32 ± 0.26	1.38
10.700	1156.3	2.02 ± 0.10	2.81	6.43 ± 0.32	1.40

TABLE II. (*Continued*)

λ	E	Krypton		Xenon	
kxu	eV	$\mu/\rho(10^3$ cm^2/g)	$\sigma(10^5$ b/atom)	$\mu/\rho(10^3$ cm^2/g)	$\sigma(10^6$ b/atom)
10.800	1145.6	2.07 ± 0.08	2.89	6.52 ± 0.25	1.42
10.900	1135.1	2.13 ± 0.08	2.96	6.62 ± 0.28	1.44
11.000	1124.8	2.17 ± 0.08	3.02	6.72 ± 0.33	1.46
11.100	1114.7	2.22 ± 0.09	3.09	6.80 ± 0.28	1.48
11.200	1104.5	2.28 ± 0.09	3.17	6.89 ± 0.32	1.50
11.300	1094.9	2.32 ± 0.09	3.23	6.98 ± 0.34	1.52
11.400	1085.3	2.38 ± 0.12	3.31	7.05 ± 0.36	1.54
11.500	1075.9	2.44 ± 0.12	3.39	7.14 ± 0.37	1.56
11.600	1066.6	2.48 ± 0.11	3.46	7.21 ± 0.40	1.57
11.700	1057.5	2.54 ± 0.13	3.54	7.29 ± 0.35	1.59
11.800	1048.5	2.60 ± 0.14	3.62	7.36 ± 0.38	1.60
11.900	1039.7	2.66 ± 0.14	3.70	7.44 ± 0.37	1.62
12.000	1031.1	2.73 ± 0.14	3.79	7.50 ± 0.32	1.64
12.100	1022.6	2.78 ± 0.12	3.87	7.57 ± 0.36	1.65
12.200	1014.2	2.84 ± 0.12	3.95	7.64 ± 0.44	1.67
12.300	1005.9	2.89 ± 0.14	4.02	7.71 ± 0.40	1.68
12.400	997.8	2.96 ± 0.16	4.11	7.79 ± 0.45	1.70
12.500	989.8	3.01 ± 0.15	4.19	7.87 ± 0.35	1.72
12.600	982.0	3.08 ± 0.16	4.28	7.93 ± 0.41	1.73
12.700	974.3	3.14 ± 0.13	4.36	8.00 ± 0.47	1.74
12.800	966.6	3.19 ± 0.16	4.44	8.11 ± 0.42	1.77
12.900	959.2	3.26 ± 0.14	4.54	8.23 ± 0.35	1.79
13.000	951.8	3.33 ± 0.14	4.63	8.34 ± 0.35	1.82
13.100	944.5	3.41 ± 0.17	4.74	8.42 ± 0.48	1.84
13.200	937.4	3.48 ± 0.15	4.84	8.52 ± 0.58	1.86
13.300	930.3	3.53 ± 0.21	4.91	8.99 ± 0.60	1.96
Xe	928.1$^+$			9.00 ± 0.54	1.96
M_{III}	928.1$^-$			7.15 ± 0.39	1.56
13.400	923.4	3.58 ± 0.18	4.98	7.17 ± 0.43	1.56
13.500	916.5	3.65 ± 0.21	5.08	7.31 ± 0.38	1.59
13.600	909.8	3.72 ± 0.25	5.18	7.47 ± 0.39	1.63
13.700	903.2	3.80 ± 0.23	5.27	7.62 ± 0.40	1.66
13.800	896.6	3.87 ± 0.19	5.38	7.79 ± 0.48	1.70
13.900	890.2	3.95 ± 0.23	5.50	7.97 ± 0.53	1.74
14.000	883.8	4.00 ± 0.25	5.57	8.14 ± 0.58	1.77
14.100	877.5	4.09 ± 0.21	5.68	8.32 ± 0.51	1.81
14.200	871.4	4.16 ± 0.28	5.79	8.51 ± 0.62	1.85
14.300	865.3	4.23 ± 0.26	5.89	8.70 ± 0.42	1.90
14.400	859.3	4.31 ± 0.22	6.00	8.82 ± 0.62	1.92
14.500	853.3	4.38 ± 0.25	6.10	9.02 ± 0.57	1.97
14.600	847.5	4.48 ± 0.26	6.23	9.34 ± 0.56	2.04
14.700	841.7	4.53 ± 0.31	6.31	9.56 ± 0.65	2.08
14.800	836.0	4.60 ± 0.28	6.40	9.78 ± 0.60	2.13
14.900	830.4	4.71 ± 0.29	6.55	10.03 ± 0.59	2.19
15.000	824.9	4.78 ± 0.28	6.66	10.34 ± 0.59	2.25

confidence limit. Columns 4 and 6 give photoelectric atomic cross sections; they have been calculated from the relations

$$\sigma = (A/N)(\mu/\rho) - \sigma_{t.\,sc.},$$

which can be written as

$$\sigma(\text{b/atom}) = 139.14\ \mu/\rho\ (\text{cm}^2/\text{g}) - \sigma_{t.\,sc.}$$

for krypton,

$$= 218.03\ \mu/\rho - \sigma_{t.\,sc.} \quad \text{for xenon,}$$

using $A = 83.80$ and 131.30 and $N = 6.0225 \times 10^{23}$.[27] $\sigma_{t.\,sc.}$ is the sum of incoherent- and coherent-scattering cross sections. Its values have been taken from the calculations of Storm and Israel[16] and McMaster *et al.*[17] Corrections due to scattering are very low, of the order of a few per thousand, except in the high-energy side of our measurement range, where they can reach 2%.

Attenuation coefficients for krypton are plotted in Fig. 1 (full energy range) and Fig. 2 (L edges energy region). The four values determined by Henke *et al.*[28] at low energy and the two measurements of McCrary *et al.*[29] at higher energy are in

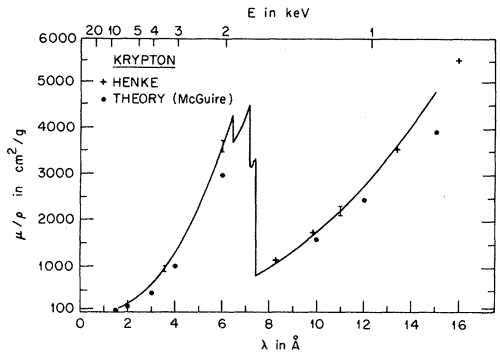

FIG. 1. Mass-attenuation coefficients in krypton. The curve was obtained by a least-squares fit of the experimental results. Error (twice the standard deviation) is indicated for a few points. The only previous measurements below 3 keV are from Henke (Ref. 28).

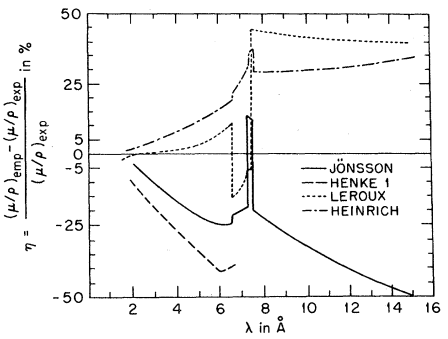

FIG. 3. Comparison of various mass-attenuation coefficient semiempirical determinations with experimental results in krypton. Good agreement is obtained in one case and only for energies higher than L_I edge energy (Leroux, Ref. 4).

excellent agreement with our results, within 2%. Agreement with McGuire's theoretical values[14] calculated by means of Herman and Skillman's model (central-field potential) is also good, usually within 10%.

The small maximum noted L_{III}-N in Fig. 2 between L_{II} and L_{III} edges is due to double excitation processes simultaneously involving $2p_{3/2}$ and $4p$ (and $4s$) electrons, followed by a double ionization continuum. These processes have been discussed in detail elsewhere.[10,18]

The expression $\log\mu/\rho$ varies linearly with $\log\lambda$ for each part of the absorption curve, which allowed us to determine from least-squares adjustment the following formulas:

$$\lambda < \lambda_{L_I}(6.45\ \text{Å}), \quad \mu/\rho_{(\text{cm}^2/\text{g})} = 31.3\,\lambda^{2.65}\ (\text{Å}),$$

$$\lambda > \lambda_{L_{III}}(7.40\ \text{Å}), \quad \mu/\rho = 5.43\,\lambda^{2.50}.$$

These formulas are to be compared with Leroux's[4] and Heinrich's[5] formulas; from experimental value compilations covering all Z range, Leroux obtained

$$\mu/\rho = 32.26\,\lambda^{2.6628} \quad \text{and} \quad 7.55\,\lambda^{2.5065},$$

and Heinrich obtained

$$\mu/\rho = 31.25\,\lambda^{2.73} \quad \text{and} \quad 5.60\,\lambda^{2.60}.$$

Jönsson[1] and Henke *et al.*[3] proposed also "universal" curves allowing attenuation-coefficient determinations. Figure 3 shows variations of the relative shift between semiempirical values and our results. For the wavelengths lower than L_I edge wavelength, Leroux's formula is the only one giving satisfactory agreement with experiments in all the energy range, within 10%. For higher wavelengths no method shows good agreement; this can be explained by lack of experimental results for krypton, when these methods were elaborated.

Attenuation coefficients for xenon are plotted in Fig. 4 (full energy range) and Fig. 5 (L edges region). Previously determined values by means of characteristic x-ray lines are more numerous than in the krypton case. At high energy, the results of White,[30] Gableske and Möring,[31] and McCrary *et al.*[29] are in very good agreement with our results. Below 2 keV the agreement with measurements of Lukirskii *et al.*[32] is within 5%, but differences between our results and results of Henke *et al.*[28] usually reach 10%. McGuire's theoretical values agree well with our measurements, within 10% in all the energy range.

No absorption jump has been detected at the calculated energy for M_I and M_{II} absorption edges. Only a small inflection of the curve is discernible at the M_{II} edge. But there is a significant increase in the attenuation coefficient close to the M_{III} edge (928.1 eV). The observed maximum at 1.6 eV from the threshold is analogous to the delayed

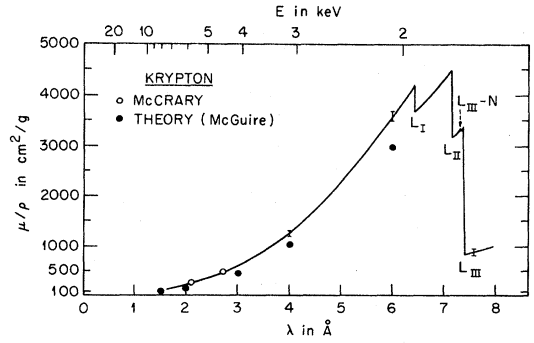

FIG. 2. Mass-attenuation coefficients in the krypton L absorption edge range. Peak labeled L_{III}-N is due to multiple excitation processes. Two values only had been previously determined above 3 keV, by McCrary (Ref. 29).

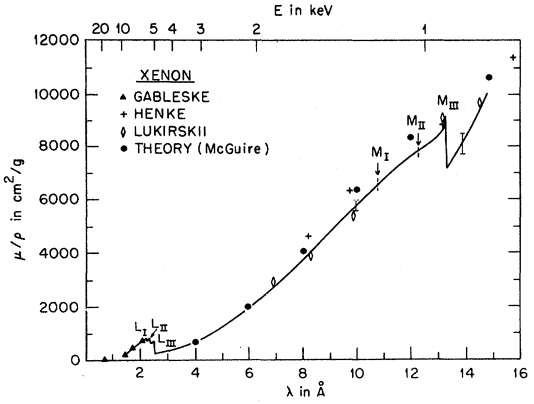

FIG. 4. Mass-attenuation coefficients in xenon. The curve was obtained by a least-squares fit of the experimental results. Error (twice the standard deviation) is indicated for one energy. Previous measurements are from Gableske and Möring (Ref. 31), Lukirskii (Ref. 32), and Henke (Ref. 28). No absorption jump was observed at the M_I and M_{II} absorption edge. A significant increasing of the attenuation coefficient close to the M_{III} edge is to be noted.

onset maxima in more outer subshell photoionization cross sections theoretically provided for by the Herman–Skillman central potential model[7,33] and experimentally observed in rare gases[34] and heavy atoms.[6] In xenon, Deslattes[35] measured such a behavior in the $3d$-subshell photoionization cross sections. As provided for by theory, the relative increase is much smaller for the inner $3p$ subshell and is located closer to the ionization threshold. Our cross-section values are in good agreement with theoretical results.[36]

Logμ/ρ varies linearly with logλ at energies higher than L_I edge energy and has been determined as

$$\mu/\rho\,(\mathrm{cm}^2/\mathrm{g}) = 94.6\lambda^{2.65}(\text{Å}) \qquad (\lambda < 2.27\ \text{Å})\ .$$

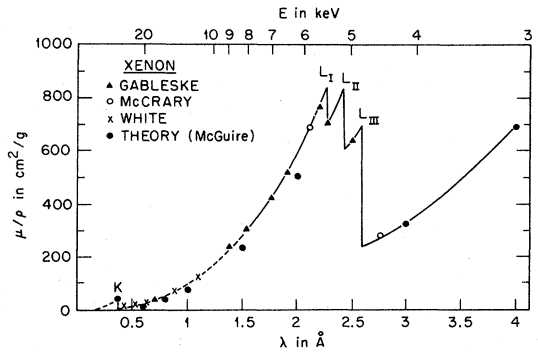

FIG. 5. Mass-attenuation coefficients in the xenon L absorption edge range. Previous experimental results are from White (Ref. 30), Gableske and Möring (Ref. 31), and McCrary (Ref. 29).

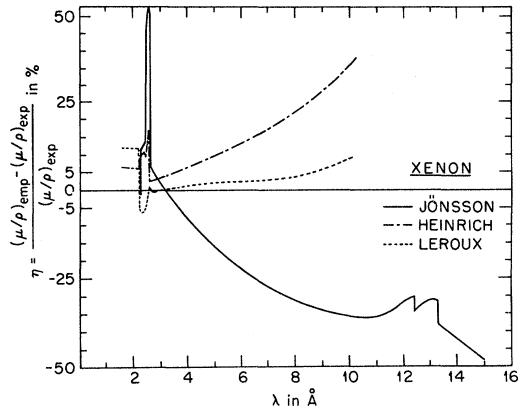

FIG. 6. Comparison of various mass-attenuation coefficient semiempirical determinations with experimental results in xenon. As in the case of krypton good agreement is obtained only for Leroux's formula.

This result is to be compared with Leroux's $\mu/\rho = 104.72\lambda^{2.6628}$ and Heinrich's $\mu/\rho = 98.30\lambda^{2.69}$. Below L_{III} edge energy, there is no more linear variation and differences with the hydrogenic model are increasing with decreasing energy.

Figure 6 shows variations of the relative shift between semiempirical values and our results. Leroux's method still gives the best results (within 10%) in the energy range where it can be used.

We also compared our results with those of McMaster *et al.*[17] and data tables of Storm and Israel,[16] both being the most extensive photoionization cross-section tables in a very large energy range. Table III shows this comparison in the form of percent differences between experimental and tabulated values; experimental values are taken as the reference. The values of McMaster *et al.* agree well with our measurements in the full energy range for krypton, and up to 2 keV for xenon. Differences with Storm and Israel's values

TABLE III. Comparison between experimental values and tabulated values. Differences $[(\mu/\rho)_{tab.} - (\mu/\rho)_{expt.}]/(\mu/\rho)_{expt.}$ are given in percent for compilations of Storm and Israel (Ref. 16) and McMaster *et al.* (Ref. 17).

	Krypton		Xenon	
E (keV)	Storm–Israel	McMaster *et al.*	Storm–Israel	McMaster *et al.*
1	+24.1	−2.1	+23.5	+44.8
1.5	+20.9	+8.9	+29.5	+13.4
2	+13.2	+1.7	+17.7	+8.5
3	+4.8	+2.3	+6.1	+6.5
4	−1.5	−1.5	+6.2	+12.9
5	−4.9	−3.0	+12.4	+6.3
6	−6.3	−3.1	+5.5	+4.0
8	−7.0	−3.5	+5.6	+4.6

TABLE IV. Absorption jump ratios in krypton and xenon.

Absorption edge	Krypton This work	Krypton McMaster[a] *et al.*	Krypton Storm–[b] Israel	Xenon This work	Xenon Wata-[c] nabe	Xenon Nore-[d] land	Xenon McMaster *et al.*	Xenon Storm–Israel
L_{I}	1.15(4)	1.16	1.14	1.18(6)	1.12(10)	1.10(5)	1.16	1.15
L_{II}	1.45(7)	1.41	1.38	1.37(17)	1.32(10)	1.31(10)	1.40	1.39
L_{III}	4.17(17)	4.15	4.77	2.84(15)	2.36(20)	2.95(20)	2.84	3.42
M_{III}				1.20(6)[e]			1.05	1.24

[a]Reference 17.
[b]Reference 16.
[c]Reference 37.
[d]Reference 38.
[e]Theoretical calculations (Ref. 36) give 1.22, in excellent agreement with this measurement.

are higher, in particular at low energy.

Table IV gives krypton and xenon L, and xenon M_{III} jump ratios, compared with other experimental or semiempirical determinations. Constant values of 1.17 and 1.39 have been estimated by Heinrich[5] for L_{I} and L_{II} jump ratios of elements with $Z > 30$, and Nordfors's[39] measured corresponding values of 1.15 and 1.38 for $47 < Z < 52$, as well as 3.06 to 2.88 for L_{III} jump ratio. Among the various xenon experimental values, our values are the closest to Heinrich's estimations and Nordfors's measurements; for krypton there is also good agreement. Tabulated values agree both for L_{I} and L_{II} jump ratios, but only McMaster's Table gives a satisfactory L_{III} value, in very good agreement with our experiment. Our M_{III} jump-ratio value also agrees well with the theoretical value calculated by Combet Farnoux.

Finally we determined the continuous oscillator strengths of krypton and xenon L shells and the xenon M shell.

Oscillator density for transitions to continuum states can be written as[40]

$$\frac{df}{dE} = \frac{mc}{\pi e^2 h}\,\sigma(E)\,.$$

Introducing wavelength in this formula and integrating, we obtain

$$f_{nc} = \frac{A}{N}\,\frac{mc^2}{\pi e^2}\int_0^{\lambda_n}\frac{1}{\lambda^2}\left(\frac{\mu}{\rho}\right)_n d\lambda\,,$$

where f_{nc} is the oscillator strength of the n shell for transitions to the continuum states, $(\mu/\rho)_n$ is the contribution of n-shell electrons to the photoelectric mass absorption coefficient, and λ_n is the n absorption edge wavelength. By graphically integrating this formula, we got $f_{Lc} = 6.8 \pm 0.3$ for krypton and 4.8 ± 0.2 for xenon. For adjacent elements ($Z = 47$ to 52), Nordfors[39] measured an averaged value of 4.7 in good agreement with the value we determined. Finally by using Deslattes's results[35] in the M_V-edge energy region, we obtained $f_{Mc} = 20.9 \pm 1.2$.

VI. CONCLUSIONS

To conclude we have determined by continuous energy analysis the mass-attenuation coefficients of krypton and xenon between 0.8 and 8 keV. Results have been compared with various semiempirical or theoretical determinations. Among these, Leroux's formula, the tabulated data of McMaster *et al.*, and McGuire's calculations have been shown to be in good agreement with our results, most of the time within 10%. Nonhydrogenic behavior of the $3p$ xenon photoionization cross section has been revealed. Krypton and xenon L and xenon M_{III} absorption jump ratios have been determined. Finally, continuous oscillator strengths of krypton and xenon L shells and the xenon M shell shell have been graphically evaluated.

ACKNOWLEDGMENTS

The author would like to thank Professor Y. Cauchois for her interest and encouragement during the course of this work. He also expresses his appreciation for the helpful discussions with Professor C. Bonnelle.

[1]E. Jönsson, thesis (Uppsala, 1928) (unpublished).
[2]J. A. Victoreen, J. Appl. Phys. 13, 95 (1943); 20, 1141 (1949).
[3]B. L. Henke, R. W. White, and B. Lundberg, J. Appl. Phys. 28, 98 (1957).
[4]J. Leroux, Advan. X-Ray Anal. 5, 153 (1961).
[5]K. F. J. Heinrich, in *The Electron Microprobe*, edited by T. D. McKinley, Heinrich, and Wittry (Wiley, New York, 1966), pp. 296–377.
[6]P. Jaegle and G. Missoni, Compt. Rend. 262B, 71 (1966); P. Jaegle, G. Missoni, and P. Dhez, Phys. Rev. Letters 18, 887 (1967); P. Jaegle, F. Combet Farnoux, P. Dhez, M. Cremonese, and G. Onori, Phys. Rev. 188, 30 (1968).
[7]F. Combet Farnoux, Compt. Rend. 264B, 1728 (1967); J. Phys. (Paris) 30, 521 (1969); S. T. Manson and J. W. Cooper, Phys. Rev. 165, 126 (1968).
[8]R. P. Madden and K. Codling, Astrophys. J. 141, 364 (1965); K. Codling, R. P. Madden, and D. L. Ederer, Phys. Rev. 155, 26 (1967); R. P. Madden, D. L.

Ederer, and K. Codling, *ibid.* 177, 136 (1969); K. Codling and R. P. Madden, Phys. Rev. A 4, 2261 (1971).

[9]A. P. Lukirskii, Izv. Akad. Nauk SSSR, Ser. Fiz. 25, 910 (1961) [Bull. Acad. Sci. USSR, Phys. Ser. 25, 923 (1961)].

[10]F. Wuilleumer, J. Phys. (Paris) 26, 776 (1965); Compt. Rend. 270B, 272 (1970).

[11]F. Wuilleumier, J. Phys. (Paris) 32, C4-88 (1971).

[12]G. Senemaud, J. Phys. (Paris) 30, 811 (1969).

[13]J. H. McCrary, E. H. Plassmann, J. M. Puckett, A. L. Conner, and G. W. Zimmermann, Phys. Rev. 153, 307 (1967).

[14]E. J. McGuire, Phys. Rev. 175, 20 (1968).

[15]F. Herman and S. Skillman, *Atomic Structure Calculations* (Prentice-Hall, Englewood Cliffs, N. J., 1963).

[16]E. Storm and H. I. Israel, Los Alamos Scientific Laboratory Report No. LA-3753, 1967 (unpublished); Nucl. Data 7A, 565 (1970).

[17]W. H. McMaster, N. K. Del Grande, J. H. Mallett, and J. H. Hubbel, Lawrence Radiation Laboratory Report No. UCRL-50174, 1969 (unpublished).

[18]F. Wuilleumier, thesis (Paris, 1969) (unpublished).

[19]C. Bonnelle, thesis (Paris, 1964) (unpublished); Ann. Phys. (Paris) 1, 439 (1966).

[20]L. G. Parrat, J. O. Porteus, H. W. Schnopper, and T. Watanabe, Rev. Sci. Instr. 30, 344 (1959).

[21]G. Brogren, Arkiv. Mat. Astron. Fysik 36, No. 3 (1948).

[22]G. Brogren and L. Haegglom, Arkiv Fysik 2, 1 (1950).

[23]M. Siegbahn, *Spectroskopie der Röntgenstrahlen*, 2nd ed. (Springer-Verlag, Berlin, 1931).

[24]P. Haglund, Arkiv Mat. Astron. Fysik 28A, No. 8 (1941).

[25]Y. Cauchois and H. Hulubei, *Tables des longueurs d'onde des Èmissions X* (Gauthier Villars, Paris, 1947).

[26]B. N. Taylor, W. H. Parker, and D. N. Langenberg, Rev. Mod. Phys. 41, 375 (1969).

[27]*Handbook of Chemistry and Physics*, 51st ed., edited by R. C. Weast (Chemical Rubber Co., Cleveland, Ohio, 1970).

[28]B. L. Henke, R. L. Elgin, R. L. Lent, and R. B. Ledingham, Norelco Reptr. 14, 112 (1967).

[29]J. H. McCrary, L. D. Looney, and C. P. Constanten, Phys. Rev. A 2, 2489 (1970).

[30]T. N. White, Phys. Rev. 46, 865 (1934).

[31]R. Gableske and M. Möring, Z. Angew. Phys. 21, 246 (1966).

[32]A. P. Lukirkii, Y. A. Brytov, and S. A. Gribovskii, Opt. i Spektroskopiya 20, 368 (1966) [Opt. Spectry (USSR) 20, 203 (1966)].

[33]U. Fano and J. W. Cooper, Rev. Mod. Phys. 40, 441 (1968).

[34]J. A. R. Samson, Adv. At. Mol. Phys. 2, 178 (1966); A. D. Lukirkii, I. A. Brytov, and T. M. Zimkina, Opt. i Spektroskopiya 17, 438 (1964) [Opt. Spectry (USSR) 17, 234 (1964)]; D. L. Ederer, Phys. Rev. Letters 13, 760 (1964); A. P. Lukirkii and T. M. Zimkina, Izv. Akad. Nauk SSSR, Ser. Fiz. 27, 327 (1963); 27, 817 (1963) [Bull. Acad. Sci. USSR, Phys. Ser. 27, 333 (1963); 27, 808 (1963)].

[35]R. Deslattes, Phys. Rev. Letters 20, 483 (1968).

[36]F. Wuilleumier and F. Combet Farnoux, Compt. Rend. 269B, 968 (1969).

[37]K. Watanabe, Phys. Rev. 137, A1380 (1965).

[38]E. Noreland, Arkiv Fysik 37, 368 (1968).

[39]B. Nordfors, Arkiv Fysik 20, 25 (1961).

[40]H. A. Bethe and E. E. Salpeter, *Quantum Mechanics of One and Two Electron Atoms* (Springer-Verlag, Berlin, 1957).